Analytical Methods

DOI: 10.1002/anie.201301894

Two-Color Probe to Monitor a Wide Range of pH Values in Cells**

Min Hee Lee, Ji Hye Han, Jae Hong Lee, Nayoung Park, Rajesh Kumar, Chulhun Kang, and Jong Seung Kim**

Intracellular pH homeostasis is crucial in various biological processes such as cell proliferation, apoptosis,[1–3] drug resistance,[4] phagocytosis,[5] and endocytosis.[6,7] The organelles of cells have various pH values, for instance, the interior of lysosomes[8,9] and endosomes[10] are slightly acidic, whereas activated mitochondria and the cytosol have slightly basic pH values.[11,12] Moreover, abnormal cellular pH values are known to be linked with inappropriate cellular functions, which are associated with many diseases including cancer,[10,13] Alzheimer's disease,[14] and others. It was recently reported that mitophagy, the specific autophagic elimination of mitochondria, involves a wide change in mitochondrial pH values (approximately pH 4–8), which is directly associated with the pathogenic state.[15] Thus, investigation of intracellular pH values and their fluctuation using high resolution microscopy would provide indispensable information to further understand the physiological and pathological processes involved in this process.

For measuring intracellular pH values, ratiometric fluorescent probes have been used the most, in which the probe has a single ionizable functional group and its emission spectrum becomes blue shifted or red shifted upon protonation or deprotonation by a change in pH.[16–18] Thereby, the ambiguity in pH determination, possibly caused by the environmental sensitivity of the fluorescence emission, can be efficiently excluded through ratiometric self-calibration of the two emission bands to allow an accurate and quantitative measurement of the intracellular pH value. However, measurement of the intracellular pH using these probes is limited by the small difference in wavelength between the two emission bands, as well as only functioning in a narrow pH range. These limitations are due to the fact that their fluorescence changes rely on the protonation or deprotonation of a single functional group. To overcome these limitations, a single small molecule with two different fluorophores, whose emission properties and working pH ranges are distinct, would be desirable. This ideal scenario, however, has rarely been reported in the field of pH sensors.[19]

Fluorescein and rhodamine fluorophores have been used extensively to measure intracellular pH values because of their excellent biocompatibility and high sensitivity under physiological conditions.[20] Under basic or neutral pH conditions, fluorescein gives strong green fluorescence (excitation/emission, 495/512 nm) when the cyclolactam ring is opened, but the emission is dramatically reduced at acidic pH, triggered by ring closure. In contrast, rhodamine displays strong red fluorescence (excitation/emission, 563/572 nm) at acidic pH because of opening of its cyclolactam ring but becomes non-fluorescent at basic or neutral pH when the ring is closed. Recently, nanoparticle or polymer-based sensors conjugated with pH-sensitive fluorescein and rhodamine dyes were reported for detecting a wide range of pH values.[21] In this context, we proposed combining fluorescein and rhodamine into one molecule, which would have contrasting fluorescence emission in response to pH changes, and therefore would be a fluorescent probe to measure a wide range of intracellular pH values.

Herein, we have synthesized and tested a chameleon-like fluorescent pH probe **1** composed of fluorescein and rhodamine (in their cyclolactam forms) linked with a diethylenetriamine spacer. The fluorescein and rhodamine moieties in probe **1** are expected to give green and red fluorescence emission at basic–neutral pH and at acidic pH, respectively. Thus, the ratio of the fluorescence intensities can respond to wide range of pH values, which could be an ideal diagnostic method to monitor the pH fluctuations in pathogenic cells.

Probe **1** was prepared by the synthetic route outlined in Scheme 1, in which the rhodamine derivative **2** was synthesized by adapting a reported procedure.[22] The reaction of compound **2** with fluorescein in the presence of EDCI and DMAP in DMF gave probe **1**. The structure of **1** was confirmed by ^{1}H NMR, ^{13}C NMR, and ESI-MS spectroscopy (Supporting Information).

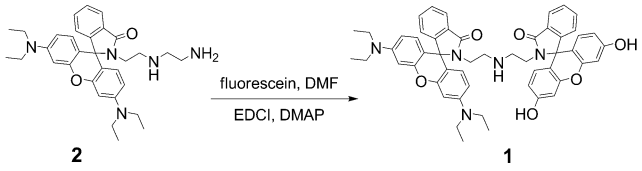

Scheme 1. Synthetic route to **1**. DMF = *N*,*N*-dimethylformamide, EDCI = 1-ethyl-3-(3-dimethylaminopropyl)carbodiimide, DMAP = 4-(dimethylamino)pyridine.

[*] M. H. Lee, J. H. Lee, N. Park, R. Kumar, Prof. J. S. Kim
Department of Chemistry, Korea University
Seoul, 136-701 (Korea)
E-mail: jongskim@korea.ac.kr
J. H. Han, Prof. C. Kang
The School of East-West Medical Science
Kyung Hee University
Yongin, 446-701 (Korea)
E-mail: kangch@khu.ac.kr

[**] This work was supported by the CRI project (20120000243, J.S.K.) and by the Basic Science Research Program (2012R1A1A2006259, C.K.) through the National Research Foundation of Korea (NRF) funded by the Ministry of Education, Science and Technology.

Supporting information for this article is available on the WWW under http://dx.doi.org/10.1002/anie.201301894.

Spectroscopic studies of probe **1** in various buffer solutions and different pH values were undertaken using UV/Vis absorption and fluorescence spectroscopy. Under basic–neutral pH conditions, probe **1** had a sharp absorption band at 495 nm and strong fluorescence emission at 512 nm. In contrast, under acidic pH conditions, probe **1** displayed a sharp absorption band at 563 nm and a strong emission band at 580 nm, however, an emission band around 512 nm is also weakly visible (Figure 1a; Supporting Information, Figure S1). The fluorescence emission bands of probe **1** at 512 nm and 580 nm in a wide pH range can be explained by the pK_a values of the ring opening–closing equilibrium of fluorescein (p$K_a = 9.2 \pm 0.12$) and rhodamine (p$K_a = 3.1 \pm 0.02$; Figures S2, S3).

The fluorescence spectral changes of **1** at various pH values (pH 3.2–10.0) are shown in Figure 1a. Increasing pH values give rise to higher fluorescence intensity of fluorescein at 512 nm (F_{512}), while the intensity of rhodamine at 580 nm (F_{580}) decreases concomitantly. An easy-to-discern fluorescent color change from orange to green was observed with increasing pH value. As seen in Figure 1b, the relative ratio of fluorescence intensities (F_{512}/F_{580}) increased by 120-fold (from 0.08 to 9.59) over the pH range of 3.2–10.0. Interestingly, we noticed that plotting the ratio (F_{512}/F_{580}) versus the pH value gives a linear relationship in pH range 4–8, which covers most of the pH ranges needed for biological applications (for example, quantitative intracellular pH measurement).

To determine any interference on the pH measurement by biological molecules, we measured the fluorescence spectra using probe **1** in the presence of essential metal ions (Na^+, K^+, Ca^{2+}, Zn^{2+}, Mg^{2+}, Mn^{2+}, Cu^{2+}, Fe^{2+}, Fe^{3+}), oxidative-stress-associated redox chemicals (including thiols; glutathione (GSH), cysteine (Cys), homocysteine (Hcy)) or H_2O_2 under physiological conditions (PBS buffer, pH 7.4, 37 °C). No appreciable spectroscopic changes were observed (Figure S4) under these conditions, which implies that probe **1** could be used to measure the intracellular pH changes without interference. In addition, as seen in Figure 1c, the fluorescence emission of probe **1** is easily reversible between pH 4–10, which enables us to propose a mechanism for the equilibrium of probe **1** with variations in pH (Scheme 2). The quantum yields (Φ_f) were also measured at different pH values (Figure S5).

Next, probe **1** was used to determine the pH value in cells using confocal microscopy (Figure 2). These images showed many spots within the cells that are presumably the organelles. Spectral analysis of HeLa cells labeled with probe **1** revealed two distinguishable emission spectra corresponding to fluorescein at 500–550 nm (green, Figure 2a,e) and rhodamine at 555–650 nm (red, Figure 2b,e). The emission maxima at 515 nm and 585 nm are in good agreement with those of probe **1** measured in vitro. As shown in the overlay image (Figure 2c), the green fluorescence is clearly distinct from that of the red fluorescence, showing that these images correspond to basic and acidic pH conditions of the organelles within HeLa cells, which is in accordance with the fluorescent response of probe **1**. Similar results were observed in HepG2 cells stained using probe **1** (Figure S6).

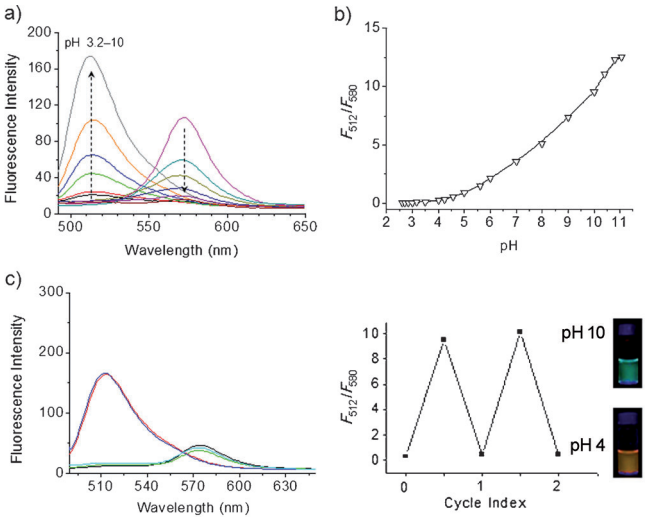

Figure 1. a) Fluorescence spectra of probe **1** (5.0 μM) at different pH values (arrows show direction of pH increase from 3.2 to 10). b) Plot of F_{512}/F_{580} versus pH value. F_{580} and F_{512} indicate the fluorescence intensity at 580 nm and at 512 nm, respectively. c) Left) reversible fluorescence changes of probe **1** between pH 4 (black, cyan, green) and pH 10 (blue, red). Right) reversible fluorescence ratio (F_{512}/F_{580}) changes between pH 4 and pH 10. All data were obtained from excitation at 480 nm in buffer solution containing 1% (*v*/*v*) DMSO at 37 °C.

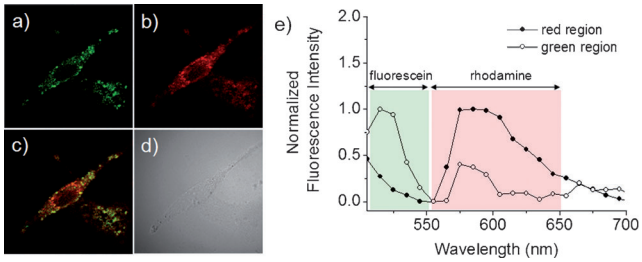

Figure 2. Confocal microscopy images of HeLa cells treated with probe **1**. Cells were incubated with PBS buffer containing probe **1** (5.0 μM) for 40 min. Cell images were then collected at a) 495–550 nm and at b) 560–650 nm. c) Overlay image of (a) and (b), and d) contrast image. e) Fluorescence spectra of the HeLa cells. All images and spectra were obtained by excitation at 488 nm.

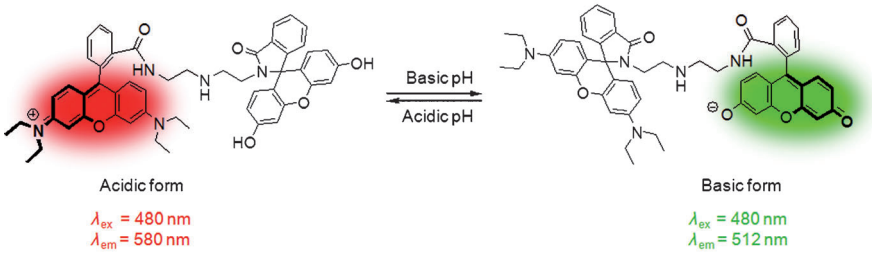

Scheme 2. Proposed mechanism for the fluorescence changes of probe **1** upon pH variation.

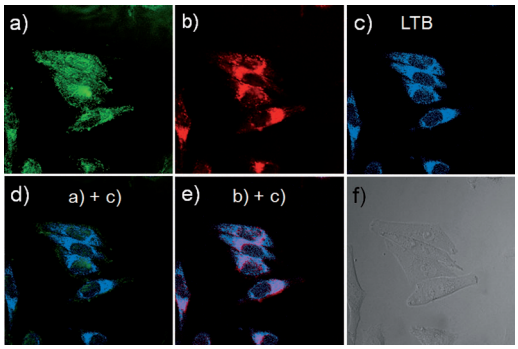

Figure 3. Colocalization experiments using probe **1** and LysoTracker Blue DND-22 (LTB) in HeLa cells. Cells were incubated with probe **1** (10.0 μM) for 40 min at 37 °C, and the medium was replaced with fresh medium containing LTB (2.0 μM) and incubated for 10 min. The excitation wavelength was 488 nm and images were collected at a) 500–545 nm and b) 560–650 nm. c) Image was obtained by using two-photon excitation at 750 nm and an emission filter of 350–475 nm. d, e) Merged images of panel (a–c), as noted. f) The corresponding contrast image.

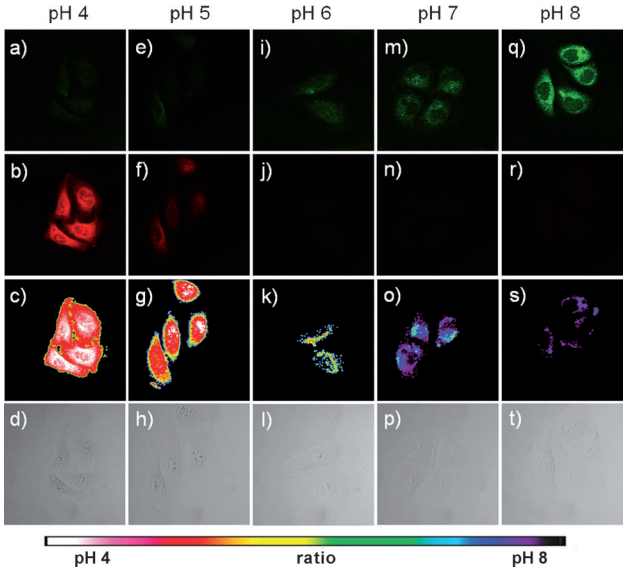

Figure 4. Confocal microscopy images of probe **1** (10.0 μM) in HeLa cells clamped at pH 4 (a–d), 5 (e–h), 6 (i–l), 7 (m–p), and 8 (q–t). The excitation wavelength was 488 nm and the images were collected at 515–545 nm (first row, fluorescein) and 565–595 nm (second row, rhodamine). Ratio images obtained from the green and red channels (third row) and the corresponding contrast images (fourth row).

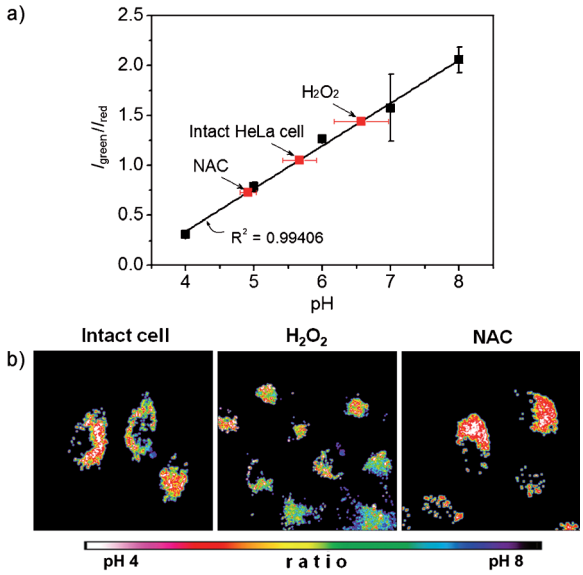

Figure 5. a) Intracellular pH calibration curve of probe **1** in HeLa cells. b) Confocal microscopy images of probe **1** (10.0 μM) loaded HeLa cells. Intact cells, H_2O_2 (0.1 mM) treated, and NAC (1.0 mM) treated cells were incubated for 1 h at 37 °C. The ratio of green (I_{green}) to red (I_{red}) fluorescence intensity of each cell is plotted in (a). The excitation wavelength was 488 nm and the ratio images were obtained from green (515–545 nm) and red (565–595 nm) channels.

Furthermore, we performed colocalization experiments using probe **1** and organelle-specific fluorescent dyes (LysoTracker Blue and MitoTracker Deep Red) to identify the intracellular location of the green and red fluorescence. The red image of probe **1** mainly overlaps with that of LysoTracker (Figure 3; Figure S7) indicating that the acidic pH (3.5–6)[8,15,21d] in lysosomes activates the ring opening of the rhodamine. However, neither LysoTracker nor MitoTracker overlapped with the green fluorescence, which suggests that the ring-opened form of fluorescein of probe **1** is not localized to lysosomes or mitochondria, but seems to be in the cytosol. From Figure 2 and 3, we infer that probe **1** can be effective for measuring a wide range of intracellular pH values in cells, including within lysosomes. Furthermore, the ratio of the fluorescence intensity from both fluorophores in probe **1** allows quantitative measurement of intracellular pH values.

For the quantification of probe **1** in HeLa cells, the intracellular pH was homogenized to the surrounding medium using the H^+/K^+ ionophore, nigericin. The fluorescence emission of the fluorescein unit (Figure 4, first row; I_{green}) in cells increases with pH value (4–8), whereas with the rhodamine unit (second row; I_{red}) it gradually decreases but was still measurable owing to a wide range of emission filters in the confocal microscope. The change in the ratio of green (I_{green}) to red (I_{red}) intensity shows the ability of probe **1** to measure a pH-dependent signal linearly over the pH range 4–8 ($R^2 = 0.99406$; Figure 5a).

To investigate the effects of the redox chemicals, such as H_2O_2 and NAC (*N*-acetylcysteine, a GSH precursor), on the acidity of the organelles, the average pH values of HeLa cells were measured (Figure 5b) based on the calibration curve in Figure 5a. The pH values for the untreated, H_2O_2, and NAC treated cells were determined to be 5.7 ± 0.2, 6.6 ± 0.4, and 4.9 ± 0.1, respectively (Figure 5a; Figure S8). This result indicates that H_2O_2 causes the organelles (possibly the lysosomes) to become more basic in HeLa cells, and that NAC has the opposite effect. More basic lysosomes caused by an oxidant is in agreement with reports that the luminal pH of lysosomes is controlled by V-ATPase[23] and that the inactivation of lysosomal V-ATPase by oxidative stress results in an increase of the lysosomal pH.[24] Also acidification of the lysosomes by GSH, presumably generated from NAC,[25]

supports the theory that a reductive cellular environment induces lysosomal activation followed by their acidification.[26] Likewise, the results in Figure 5 clearly demonstrated that the intracellular oxido-redox balance could control the acidity of the lysosomes. In addition, these trends in intracellular pH value in the presence of redox chemicals (NAC, H_2O_2) are supported by comparative experiments with the commercially available LysoSensor Yellow/Blue DND-160, confirming the validity of our pH probe (Figure S9).

In summary, a chameleon fluorescent pH probe composed of both fluorescein and rhodamine units was synthesized in high yield and used to visualize organelles in cells having different pH values. We observed that the cyclolactam rings of rhodamine and fluorescein open in acidic and in neutral–basic media to give fluorescence emission at 580 and 512 nm, respectively. We also found that a plot of the ratio F_{512}/F_{580} versus acidity in the pH range 4–8 was linear, which covers most physiological pH values. Confocal microscopic images of HeLa cells labeled with probe **1** revealed two distinct emission ranges at 500–550 nm (green) and at 555–650 nm (red), corresponding to neutral–basic and acidic organelles within the cell, respectively. Colocalization experiments confirmed that the red fluorescence of probe **1** overlapped with a lysosomal dye and the green fluorescence corresponded to basic organelles in the cytoplasm. From the pH-dependent calibration curve of the fluorescence changes of probe **1**, the lysosomal pH value of HeLa cells was estimated to be 5.7 ± 0.2, which could be changed by adding H_2O_2 or NAC. This lead us to conclude that the pH value of the lysosomes could be controlled by the cellular redox balance. Therefore, probe **1** gives a dramatic change in the relative fluorescence intensity of its two fluorophores over a wide pH range and could be an ideal diagnostic method for measuring pH fluctuations in pathogenic cells.

Received: March 6, 2013
Revised: March 22, 2013
Published online: April 22, 2013

Keywords: fluorescein · fluorescent probes · imaging agents · intracellular pH · rhodamine

[1] D. Perez-Sala, D. Collado-Escobar, F. Mollinedo, *J. Biol. Chem.* **1995**, *270*, 6235.
[2] A. Ishaque, M. Al-Rubeai, *J. Immunol. Methods* **1998**, *221*, 43.
[3] R. A. Gottlieb, J. Nordberg, E. Skowronski, B. M. Babior, *Proc. Natl. Acad. Sci. USA* **1996**, *93*, 654.
[4] S. Simon, D. Roy, M. Schindler, *Proc. Natl. Acad. Sci. USA* **1994**, *91*, 1128.
[5] M. Miksa, H. Komura, R. Wu, K. G. Shah, P. Wang, *J. Immunol. Methods* **2009**, *342*, 71.
[6] M. Lakadamyali, M. J. Rust, H. P. Babcock, X. Zhuang, *Proc. Natl. Acad. Sci. USA* **2003**, *100*, 9280.
[7] E. J. Adie, S. Kalinka, L. Smith, M. J. Francis, A. Marenghi, M. E. Cooper, M. Briggs, N. P. Michael, G. Milligan, S. Game, *BioTechniques* **2002**, *33*, 1152.
[8] S. Ohkuma, B. Poole, *Proc. Natl. Acad. Sci. USA* **1978**, *75*, 3327.
[9] A. Abiko, S. Masamune, *Tetrahedron Lett.* **1996**, *37*, 1081.
[10] M. Schindler, S. Grabski, E. Hoff, S. Simon, *Biochemistry* **1996**, *35*, 2811.
[11] C. Balut, M. vande Ven, S. Despa, I. Lambrichts, M. Ameloot, P. Steels, I. Smets, *Kidney Int.* **2008**, *73*, 226.
[12] J. Llopis, J. M. Mccaffery, A. Miyawaki, M. G. Farquhar, R. Y. Tsien, *Proc. Natl. Acad. Sci. USA* **1998**, *95*, 6803.
[13] H. Izumi, T. Torigoe, H. Ishiguchi, H. Uramoto, Y. Yoshida, M. Tanabe, T. Ise, T. Murakami, T. Yoshida, M. Nomoto, K. Kohno, *Cancer Treat. Rev.* **2003**, *29*, 541.
[14] T. A. Davies, R. E. Fine, R. J. Johnson, C. A. Levesque, W. H. Rathbun, K. F. Seetoo, S. J. Smith, G. Strohmeier, L. Volicer, L. Delva, E. R. Simons, *Biochem. Biophys. Res. Commun.* **1993**, *194*, 537.
[15] R. J. Youle, D. P. Narendra, *Nat. Rev. Mol. Cell Biol.* **2011**, *12*, 9.
[16] J. Han, K. Burgess, *Chem. Rev.* **2010**, *110*, 2709.
[17] T. Myochin, K. Kiyose, K. Hanaoka, H. Kojima, T. Terai, T. Nagano, *J. Am. Chem. Soc.* **2011**, *133*, 3401.
[18] B. Tang, F. Yu, P. Li, L. Tong, X. Duan, T. Xie, X. Wang, *J. Am. Chem. Soc.* **2009**, *131*, 3016.
[19] a) C. Percivalle, T. Mahmood, S. Ladame, *Med. Chem. Commun.* **2013**, *4*, 211; b) L. Yuan, W. Lin, Z. Cao, J. Wang, B. Chen, *Chem. Eur. J.* **2012**, *18*, 1247; c) H.-S. Peng, J. A. Stolwijk, L.-N. Sun, J. Wegener, O. S. Wolfbeis, *Angew. Chem.* **2010**, *122*, 4342; *Angew. Chem. Int. Ed.* **2010**, *49*, 4246.
[20] a) N. Klonis, W. H. Sawyer, *J. Fluoresc.* **1996**, *6*, 147; b) V. Zanker, W. Peter, *Chem. Ber.* **1958**, *91*, 572.
[21] a) H. N. Kim, M. H. Lee, H. J. Kim, J. S. Kim, J. Yoon, *Chem. Soc. Rev.* **2008**, *37*, 1465; b) W. Shi, X. Li, H. Ma, *Angew. Chem.* **2012**, *124*, 6538; *Angew. Chem. Int. Ed.* **2012**, *51*, 6432; c) L. Albertazzi, B. Storti, L. Marchetti, F. Beltram, *J. Am. Chem. Soc.* **2010**, *132*, 18158; d) S. Wu, Z. Li, J. Han, S. Han, *Chem. Commun.* **2011**, *47*, 11276.
[22] M. H. Lee, S. W. Lee, S. H. Kim, C. Kang, J. S. Kim, *Org. Lett.* **2009**, *11*, 2101.
[23] a) G.-H. Sun-Wada, Y. Wada, M. Futai, *Cell Struct. Funct.* **2003**, *28*, 455; b) D. Brown, S. Breton, *J. Exp. Biol.* **2000**, *203*, 137.
[24] a) Y. Feng, M. Forgac, *J. Biol. Chem.* **1994**, *269*, 13224; b) Y. Wang, E. Floor, *J. Neurochem.* **1998**, *70*, 646; c) D. S. Kaufman, M. S. Goligorsky, E. P. Nord, M. L. Graber, *Arch. Biochem. Biophys.* **1993**, *302*, 245; d) C.-S. Chen, *BMC Cell Biol.* **2002**, *3*, 21.
[25] C. Y. Yim, J. B. Hibbs, Jr., J. R. McGregor, R. E. Galinsky, W. E. Samlowski, *J. Immunol.* **1994**, *152*, 5796.
[26] A. Sliwa-Jozwik, A. Jozwik, W. Fronczyk, A. Guszkiewicz, A. Kolataj, *Anim. Sci. Pap. Rep.* **2004**, *22*, 237.

